Selective killing of p53-deficient cancer cells by SP600125

*Mohamed Jemaà[1,2,3†], Ilio Vitale[1,2,3†], Oliver Kepp[1,2,3], Francesco Berardinelli[4], Lorenzo Galluzzi[1,2,3], Laura Senovilla[1,2,3], Guillermo Mariño[1,2,3], Shoaib Ahmad Malik[1,2,3], Santiago Rello-Varona[1,2,3], Delphine Lissa[1,2,3], Antonio Antoccia[4], Maximilien Tailler[1,2,3], Frederic Schlemmer[1,2,3], Francis Harper[5], Gérard Pierron[5], Maria Castedo[1,2,3], Guido Kroemer[1,6,7,8,9]**

Keywords: caspases; HCT 116; high-throughput screening; mitochondrial outer membrane permeabilization; MPS1

DOI 10.1002/emmm.201200228

Received October 14, 2011
Revised January 16, 2012
Accepted February 02, 2012

The genetic or functional inactivation of p53 is highly prevalent in human cancers. Using high-content videomicroscopy based on fluorescent *TP53*$^{+/+}$ and *TP53*$^{-/-}$ human colon carcinoma cells, we discovered that SP600125, a broad-spectrum serine/threonine kinase inhibitor, kills p53-deficient cells more efficiently than their p53-proficient counterparts, *in vitro*. Similar observations were obtained *in vivo*, in mice carrying p53-deficient and -proficient human xenografts. Such a preferential cytotoxicity could be attributed to the failure of p53-deficient cells to undergo cell cycle arrest in response to SP600125. *TP53*$^{-/-}$ (but not *TP53*$^{+/+}$) cells treated with SP600125 became polyploid upon mitotic abortion and progressively succumbed to mitochondrial apoptosis. The expression of an SP600125-resistant variant of the mitotic kinase MPS1 in *TP53*$^{-/-}$ cells reduced SP600125-induced polyploidization. Thus, by targeting MPS1, SP600125 triggers a polyploidization program that cannot be sustained by *TP53*$^{-/-}$ cells, resulting in the activation of mitotic catastrophe, an oncosuppressive mechanism for the eradication of mitosis-incompetent cells.

INTRODUCTION

The genetic or functional inactivation of the tumour suppressor p53 is (one of) the most frequent molecular characteristic(s) of human cancer (Cheok et al, 2011). It has been estimated that nowadays 11 million people are living with a cancer that contains an inactivating mutation of *TP53* and additional 11 millions have neoplasms in which the p53 pathway is interrupted due to defects in the molecules that act either upstream or downstream of p53 (Brown et al, 2009).

p53 has recently been shown to control cellular homeostasis via multiple mechanisms (Vousden & Ryan, 2009). Still, p53 is best known as the major mediator of the cellular response to stress, a phenomenon that entails both transcriptional (nuclear) and non-transcriptional (cytoplasmic) p53 functions (Green & Kroemer, 2009; Vousden & Prives, 2009). Thus, in response to adverse conditions, p53 can stimulate the execution of apoptotic cell death, mainly through the transactivation of several pro-apoptotic genes (Beckerman & Prives, 2010) or physical interactions with proteins that regulate mitochondrial outer membrane permeabilization (Galluzzi et al, 2011a). Alternatively, stress-activated p53 can arrest the cell cycle, either by transactivating inhibitors of cyclin-dependent kinases or, perhaps, by direct interactions with essential cell cycle regulators (Tritarelli et al, 2004). Therefore, p53-deficient cells are notoriously resistant against the induction of apoptosis (Cheok et al, 2011) and fail to undergo cell cycle arrest in

(1) INSERM, U848, Villejuif, France
(2) Institut Gustave Roussy, Villejuif, France
(3) Université Paris Sud/Paris XI, Le Kremlin Bicêtre, France
(4) Dipartimento Di Biologia, Università Roma Tre, Rome, Italy
(5) CNRS, UMR8122, Villejuif, France
(6) Metabolomics Platform, Institut Gustave Roussy, Villejuif, France
(7) Centre de Recherche des Cordeliers, Paris, France
(8) Pôle de Biologie, Hôpital Européen Georges Pompidou, AP-HP, Paris, France
(9) Faculté de Médecine, Université Paris Descartes, Sorbonne Paris Cité, Paris, France
***Corresponding author:** Tel: +33 1 42 11 60 46; Fax: +33 1 4211 6047; E-mail: kroemer@orange.fr

†These authors contributed equally to this work.

© 2012 EMBO Molecular Medicine

response to DNA damaging agents, implying that they become genomically instable (Talos & Moll, 2010). The absence of p53 reportedly favours spontaneous tetraploidization in several distinct contexts (Davoli & de Lange, 2011; Ganem et al, 2007). Moreover, in response to mitotic inhibitors such as microtubular poisons, p53-incompetent cells can override mitotic checkpoints and hence can become polyploid, a property that is thought to contribute to chromosomal instability (Aylon et al, 2006; Finkin et al, 2008; Ha et al, 2007; Vitale et al, 2010) as well as to resistance to chemo- and radiotherapy (Castedo et al, 2006; Galluzzi et al, 2011b; Shen et al, 2008).

Thus, p53 plays a prominent role in coupling the effects of DNA damaging agents (such as ionizing radiations or chemicals including platinum derivatives and topoisomerase inhibitors) to the therapeutic induction of senescence or apoptosis. Given the prevalence and functional impact of p53 defects, many groups have attempted to identify pharmacological agents that preferentially kill p53-incompetent cells (Brown et al, 2009). While some of these compounds directly interact with mutant p53 proteins and reestablish their functions via conformational effects (Athar et al, 2011; Selivanova, 2010; Wiman, 2010), others were designed to inhibit the p53-targeting ubiquitin ligase HDM2, leading to increased p53 concentrations (Shangary & Wang, 2009). Moreover, some agents kill p53-deficient cancer cells based on their increased tendency to undergo polyploidization. VX-680 (an inhibitor of Aurora kinases) causes the endoreplication of p53-deficient cells, resulting in their death (Gizatullin et al, 2006). A combination of irradiation and BI-2536 (a inhibitor of Polo-like kinase 1, PLK1) kills *TP53*$^{-/-}$ cells more efficiently than their *TP53*$^{+/+}$ counterparts (Sur et al, 2009), and the selective toxicity of GSK461364A (another PLK1 inhibitor) against p53-deficient cells has been attributed to their failure to undergo cell cycle arrest at a tetraploid stage (Degenhardt et al, 2010). Similarly, 7-hydroxystaurosporine (UCN-01, an inhibitor of the checkpoint kinase CHEK1) has been shown to abrogate DNA damage-induced cell cycle arrest selectively in p53-defective cancer cells (Levesque et al, 2005).

In this study, we launched yet another attempt to identify compounds that kill p53-deficient cells more efficiently than their p53-positive counterparts. Using a novel videomicroscopic assay, we identified SP600125 as an agent whose cytotoxicity is exacerbated in conditions in which p53 is deleted, depleted or inhibited, *in vitro* and *in vivo*. The mechanisms through which SP600125 mediates these effects involve the selective polyploidization of p53-deficient cells due to the inhibition of the mitotic kinase MPS1. Preferentially in the context of p53 deficiency, this results in abortive mitosis, followed by the activation of mitotic catastrophe and cell death via the mitochondrial pathway of apoptosis.

RESULTS AND DISCUSSION

Identification of SP600125 as a selective inhibitor of p53-deficient cells

p53-deficient (*TP53*$^{-/-}$) human colon carcinoma HCT 116 cells or their p53-proficient wild-type (WT) counterparts stably expressing red fluorescent protein (RFP)- or green fluorescent protein (GFP)-tagged histone 2B, respectively, were co-cultured in 96-well plates for 48 h in the absence or presence of 480 distinct compounds from the ICCB library of bioactive agents. Throughout this period, the ratio of green WT *versus* red *TP53*$^{-/-}$ HCT 116 cells was quantitatively monitored by videomicroscopy. In line with the fact that p53 often mediates the cytotoxic effects of DNA-damaging agents, 10-hydroxycamptothecin and cisplatin depleted more efficiently WT than *TP53*$^{-/-}$ cells. In contrast SP600125, a broad-spectrum inhibitor of serine/threonine kinases including Aurora kinase A ($IC_{50} = 60$ nM) and B (190 nM), CDC7/DBF4 (1.59 μM), CDK2/CYCA (880 nM), CK2 (650 nM), FLT3 (90 nM), Haspin (510 nM), IKK2 (1 μM), JAK3 (410 nM), KIT (870 nM), MELK (110 nM), PDK1 (1.06 μM), PIM2 (1.05 μM), RET (1.09 μM), SYK (1.8 μM), TRKA (70 nM), TYK2 (880 nM) and VEGFR3 (300 nM) (Colombo et al, 2010), but best known for inhibiting c-Jun N-terminal kinases (JNK) 1–3 (100–200 nM) (Bennett et al, 2001; Heo et al, 2004) and MPS1 (IC_{50} 1.95 μM) (Chu et al, 2008; Schmidt et al, 2005), was the most efficient agent in increasing the ratio between WT and *TP53*$^{-/-}$ cells (Fig 1A–C). These results are consistent with previous observations (Mingo-Sion et al, 2004), and were validated using two alternative methods for measuring cell proliferation and death, namely the xCELLigence® system, which quantifies the impedance of adherent cells (Fig 1D), and cytofluorometry (Fig 1E) (Castedo et al, 2002; Galluzzi et al, 2009, 2007). Upon co-staining with the vital dye propidium iodide (PI) and the mitochondrial transmembrane potential ($\Delta\psi_m$) sensor $DiOC_6(3)$, the frequency of dying ($DiOC_6(3)^{low}$ PI^-) and dead ($DiOC_6(3)^{low}$ PI^+) cells was markedly increased among SP600125-treated *TP53*$^{-/-}$ cells but less so among WT control cells (Fig 1E). Altogether, these results suggest that SP600125 is endowed with the capacity of selectively killing p53-deficient tumour cells.

Polyploidization of p53-deficient cells responding to SP600125

Since SP600125 can perturb mitosis and/or induce endoreplication (Kim et al, 2010; Schmidt et al, 2005) we investigated its effect on the cell cycle of WT and *TP53*$^{-/-}$ HCT 116 cells. WT cells treated with SP600125 progressively acquired a 4*n* DNA content (which corresponds to the normal amount of DNA in the G_2 or M phase of the cell cycle), while *TP53*$^{-/-}$ cells accumulated a higher DNA content (8*n* or 16*n*), indicating that they became tetraploid or higher-order polyploid (Fig 2A and B). Accordingly, SP600125 blocked the incorporation of the thymidine analog 5-ethynyl-2′-deoxyuridine (EdU) into DNA in WT but not in *TP53*$^{-/-}$ cells. Moreover, at odds with their WT counterparts, *TP53*$^{-/-}$ cells continued to incorporate EdU even when they possessed a 4*n* or 8*n* DNA content (Fig 2C). A significant fraction of *TP53*$^{-/-}$ (but not WT) cells exhibited histone H3 phosphorylation, an indicator of ongoing mitosis, or stained positively for the mitotic-specific phosphoepitope MPM2 at the 8*n* stage (Fig 2D and Fig S1 of Supporting Information), Moreover, in response to SP600125, WT (but not *TP53*$^{-/-}$) cells exhibited a marked decline in cyclin B (the cyclin associated with the G_2/M phase) levels and increased amounts of cyclin E

 © 2012 EMBO Molecular Medicine

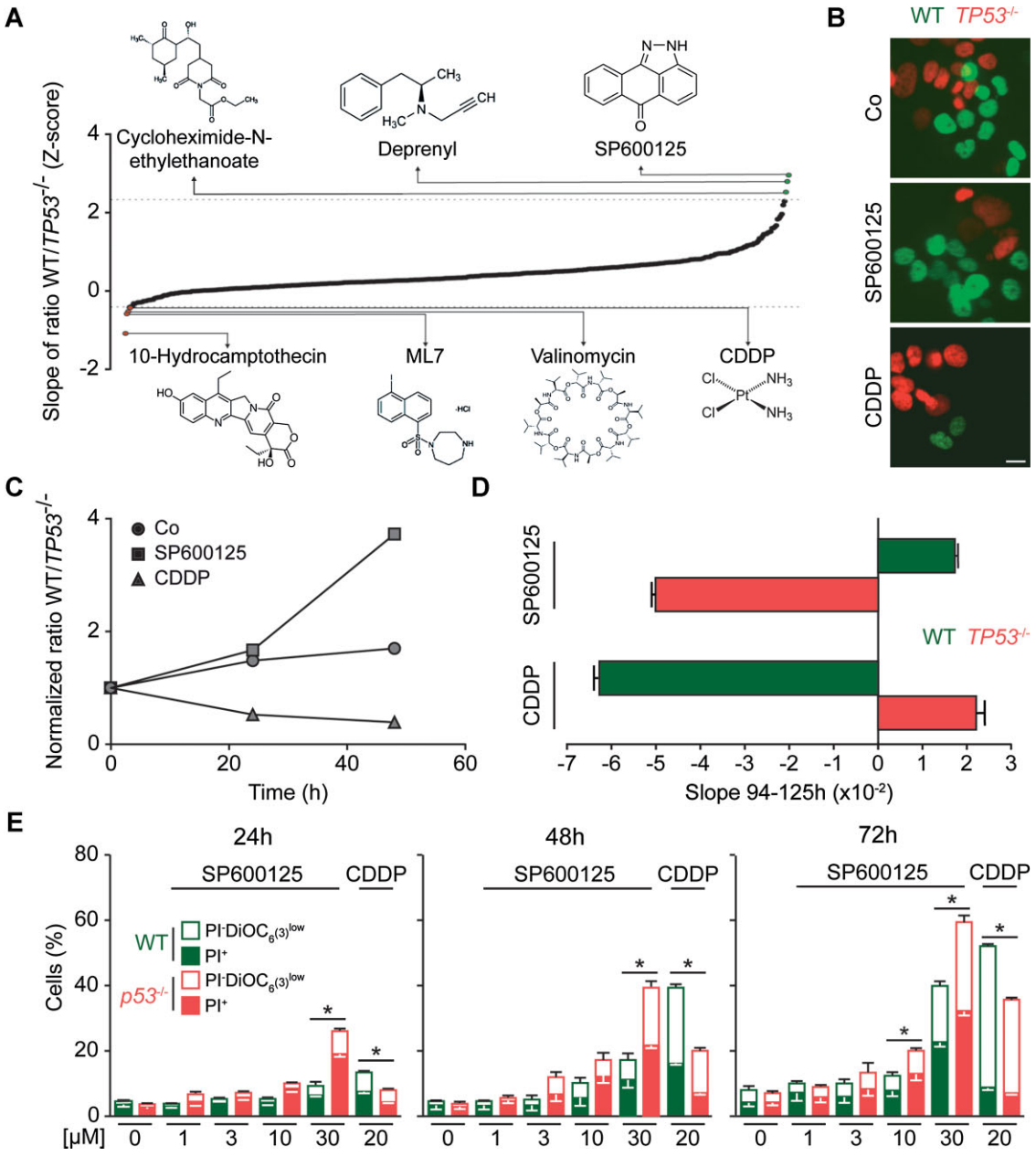

Figure 1. Identification of SP600125 as a selective inhibitor of p53-deficient cells.

A-C. Screening of the ICCB Known Bioactives Library on WT (GFP-H2B-expressing) and *TP53*$^{-/-}$ (RFP-H2B-expressing) human colon carcinoma HCT 116 cells. Cells were co-cultured at an initial 1:1 ratio in the absence (Co) or presence of 480 distinct signal transduction inhibitors and the capacity of the agents to change the ratio between GFP and RFP-labelled cells was assessed over 48 h by epifluorescence videomicroscopy. The Z-score analysis for all 480 components is reported in (**A**), snapshots taken at 48 h are shown in (**B**) (scale bar = 10 μm) and representative changes in the WT/*TP53*$^{-/-}$ cell ratio upon 30 μM SP600125 or 20 μM cisplatin (CDDP) administration are depicted in (**C**).

D,E. Confirmation of the preferential effect of SP600125 on *TP53*$^{-/-}$ cells. HCT 116 cells with the indicated genotype were cultured on plates that allow for the real-time measurement of impedance of adherent cells (for more details refer to Materials and Methods Section), in the presence or absence of 30 μM SP600125, and the slope of the growth curve was determined for triplicates ± SEM (**D**). Alternatively, cells left were left untreated or incubated with the indicated concentration of SP600125 or CDDP for the indicated time, followed by cytofluorometry for the assessment of cell death-related parameters. Green/red and black columns illustrate the percentage of dying (PI^- $DiOC_6(3)^{low}$) and dead (PI^+) cells, respectively (means ± SEM; $n = 9$). $^*p < 0.05$ (Student's *t*-test).

 © 2012 EMBO Molecular Medicine

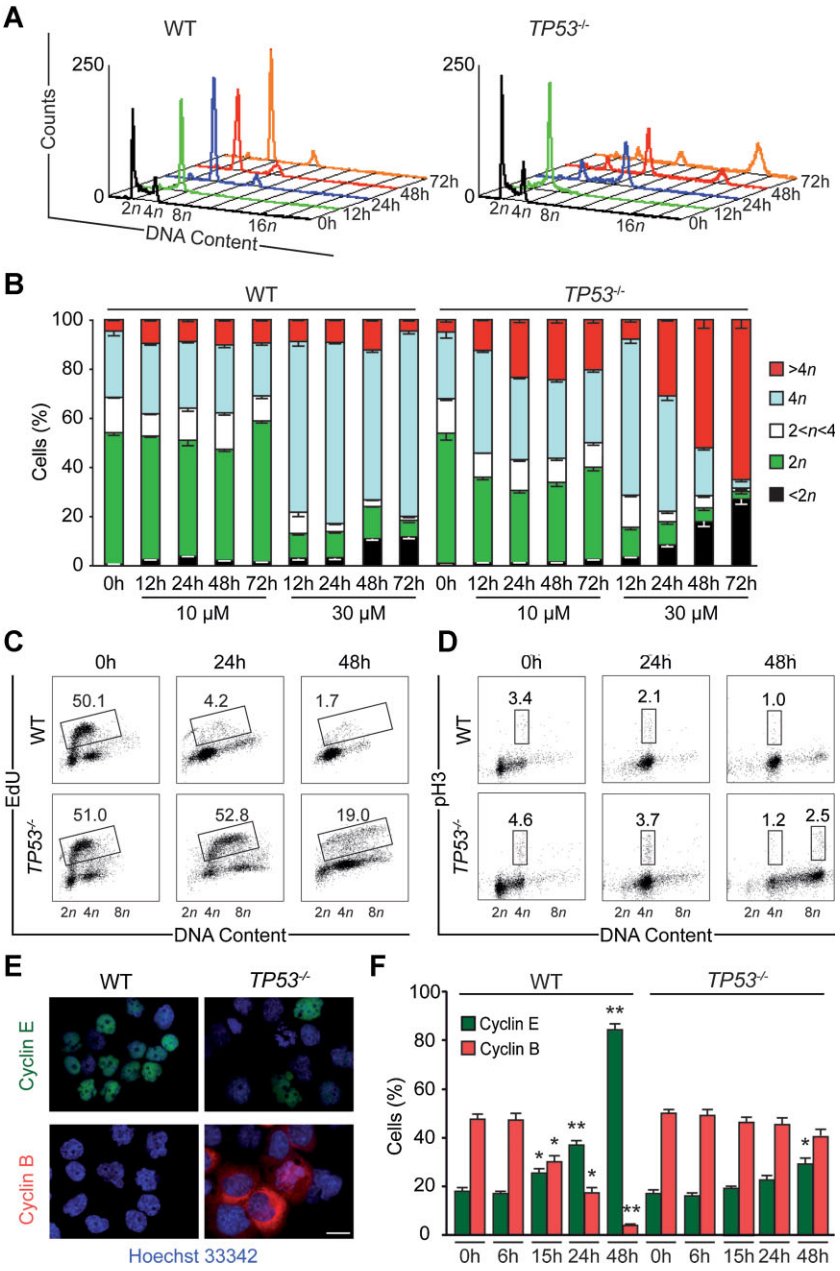

Figure 2. Selective polyploidization of p53-deficient cells in response to SP600125.

A,B. Cell cycle analysis. WT and *TP53*$^{-/-}$ human colon carcinoma HCT 116 cells were exposed to the indicated dose of SP600125 (30 μM where not specified) for the indicated time, followed by the assessment of cell cycle distribution. Panel (**A**) reports representative cell cycle distributions, panel (**B**) depicts quantitative data (means ± SEM; $n = 9$).

C-F. Paradoxical antiproliferative effects of SP600125. p53-proficient and p53-deficient cells were cultured in the presence of 30 μM SP600125 as indicated and either labelled with the thymidine analogue EdU during the last 30 min of the assay, followed by fixation and detection of EdU fluorescence (**C**) or subjected to the immunodetection of phospho-histone H3 (pH3) (**D**). PI was used to label DNA prior to cytofluorometric acquisitions. Numbers indicate the percentage of cells found in each gate. Alternatively, WT and *TP53*$^{-/-}$ cells were stained for the detection of cyclin B (in red) and cyclin E (in green) (**E** and **F**). Representative immunofluorescence microphotographs of cells treated with SP600125 for 48 h are shown in (**E**) (scale bar = 10 μm), while quantitative results (means ± SEM; $n = 3$) are reported in (**F**). $^{*}p < 0.05$ and $^{**}p < 0.01$ (Student's *t*-test), as compared to cells of the same genotype left untreated.

(the cyclin associated with the G_1/S phase) (Fig 2E and F and Fig S2 of Supporting Information). Moreover, in response to SP600125, the mitotic index (MI; *i.e.*, the fraction of cells that manifest morphological signs of mitosis) decreased more rapidly in WT cells than in their *TP53*$^{-/-}$ counterparts (Fig 3A). SP600125 indistinguishably induced the disappearance of anaphases and telophases in WT and *TP53*$^{-/-}$ cells (Fig 3A), suggesting that, in the continuative presence of SP600125, *TP53*$^{-/-}$ cells underwent abortive mitoses. Accordingly, in response to SP600125, metaphases became disorganized in both WT and *TP53*$^{-/-}$ cells, as SP600125 abolished the spindle assembly checkpoint (SAC), stimulated the degradation of cyclin B in cells with morphologically evident metaphases, and increased the number of centrosomes per cell (Fig 3B and C and Fig S3 of Supporting Information).

These results suggest that SP600125 augments the DNA content (preferentially of *TP53*$^{-/-}$ cells) in the absence of normal mitotic chromosome separation, nuclear division (karyokinesis) and daughter cell formation (cytokinesis). Accordingly, interphase FISH indicates that the SP600125-mediated increase in DNA content is not accompanied by a proportional increase in chromosome number but entails a higher hybridization signal, suggesting chromatid segregation failure (Fig 3D and E). In line with these observations, HCT 116 cells in which one single chromosome locus is labelled by GFP (because that locus contains multiple *lacO* copies that are stained by transgene-

 © 2012 EMBO Molecular Medicine

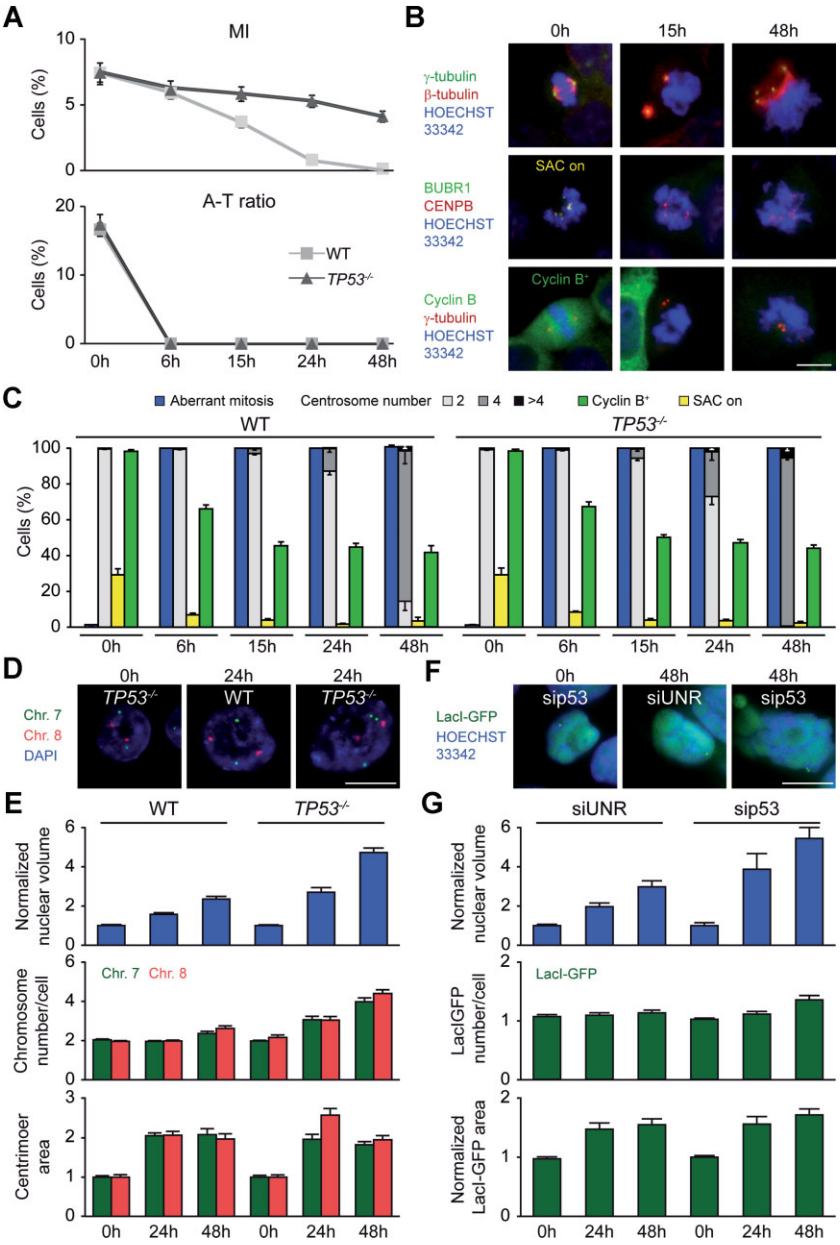

Figure 3. p53-modulated effects of SP600125 on mitotic execution.

A. Mitotic progression in SP600125-treated WT or *TP53*$^{-/-}$ cells. The total frequency of mitoses (MI) and the proportion of anaphases plus telophases among mitotic figures (A–T ratio) as determined by immunofluorescent microscopy are shown in human colon carcinoma HCT 116 cells exposed to 30 μM SP600125 for the indicated time (means ± SEM; $n = 5$).

B,C. Functional and morphological characterization of metaphases upon SP600125 treatment. Representative immunofluorescence micrographs of mitoses in *TP53*$^{-/-}$ cells treated with 30 μM SP600125 for the indicated time are shown in (**B**) and quantitative data are reported in (**C**) (means ± SEM; $n = 4$). Centrosomes and kinetochores are visualized with antibodies that recognize γ tubulin and CENP-B, respectively. The activation of the SAC is monitored by the localization at kinetochore of BUBR1. Please note that in (**C**) only (pro-) metaphases were quantified.

D,E. Interphase FISH of SP600125-treated WT or *TP53*$^{-/-}$ HCT 116 cells. Representative images of WT and *TP53*$^{-/-}$ cells treated with 30 μM SP600125 for 24 h are shown in (**D**). Panel (**E**) reports the nuclear volume (normalized to that of untreated cells), the copy number of chromosome 7 (in green) and 8 (in red) per cells, and the centromere hybridization signal area for chromosomes 7 and 8 (normalized to those of untreated cells), as determined by computerized image analyses (means ± SEM, $n = 100$ cells) (**E**).

F-G. Effect of SP600125 and p53 on HCT 116 cells that contain one single GFP-labelled chromosome (LacI-GFP). Panel (**F**) shows representative images of WT HCT 116 cells treated with 30 μM SP600125 for 48 h, either in control conditions (siUNR) or upon the siRNA-mediated p53 knockdown (sip53). Quantitative data on nuclear volume, number of LacI-GFP spots/per cell and LacI-GFP signal area (normalized to that of untreated cells) are shown in (**G**) (means ± SEM, $n = 100$ cells). Please note that the nuclear volume in (**E**) and (**G**) is directly proportional to ploidy. Scale bar = 10 μm.

expressed LacI-GFP) (Thompson & Compton, 2010) responded to SP600125 with an increase in DNA content that was not paralleled by an increase in chromosome number, in particular upon siRNA-mediated depletion of p53 (Fig 3F and G and Fig S4A of Supporting Information). In this system, chromosomal GFP labelling became more intense, further suggesting that SP600125 induces chromatin duplication in the absence of chromosomal separation.

Involvement of MPS1 in the preferential cytotoxicity of SP600125 against p53-deficient cells

Next, we investigated whether the effects of SP600125 depend on the inhibition of MPS1 or are mediated by off-target mechanisms. Transfection-enforced expression of WT MPS1 and more so of an SP600125-refractory MPS1 variant (MPS1-M602Q) (Schmidt et al, 2005), reduced the capacity of SP600125 to trigger polyploidization in *TP53*$^{-/-}$ cells (Fig 4A and B and Fig S4B of Supporting Information). The overexpression of MPS1 (and more so of MPS1-M602Q) also reduced the frequency of SP600125-treated *TP53*$^{-/-}$ cancer cells manifesting polyploid S phases and mitoses (Fig 4A, C and D) and staining positively for cyclin B (Fig 4E). In line with the interpretation that SP600125 mediates its effects (at least in part) by inhibiting MPS1, we observed that the siRNA-mediated depletion of MPS1 induced polyploidization more efficiently in *TP53*$^{-/-}$ cells than in their WT counterparts (Fig 4F and G and Fig S4C of

 © 2012 EMBO Molecular Medicine

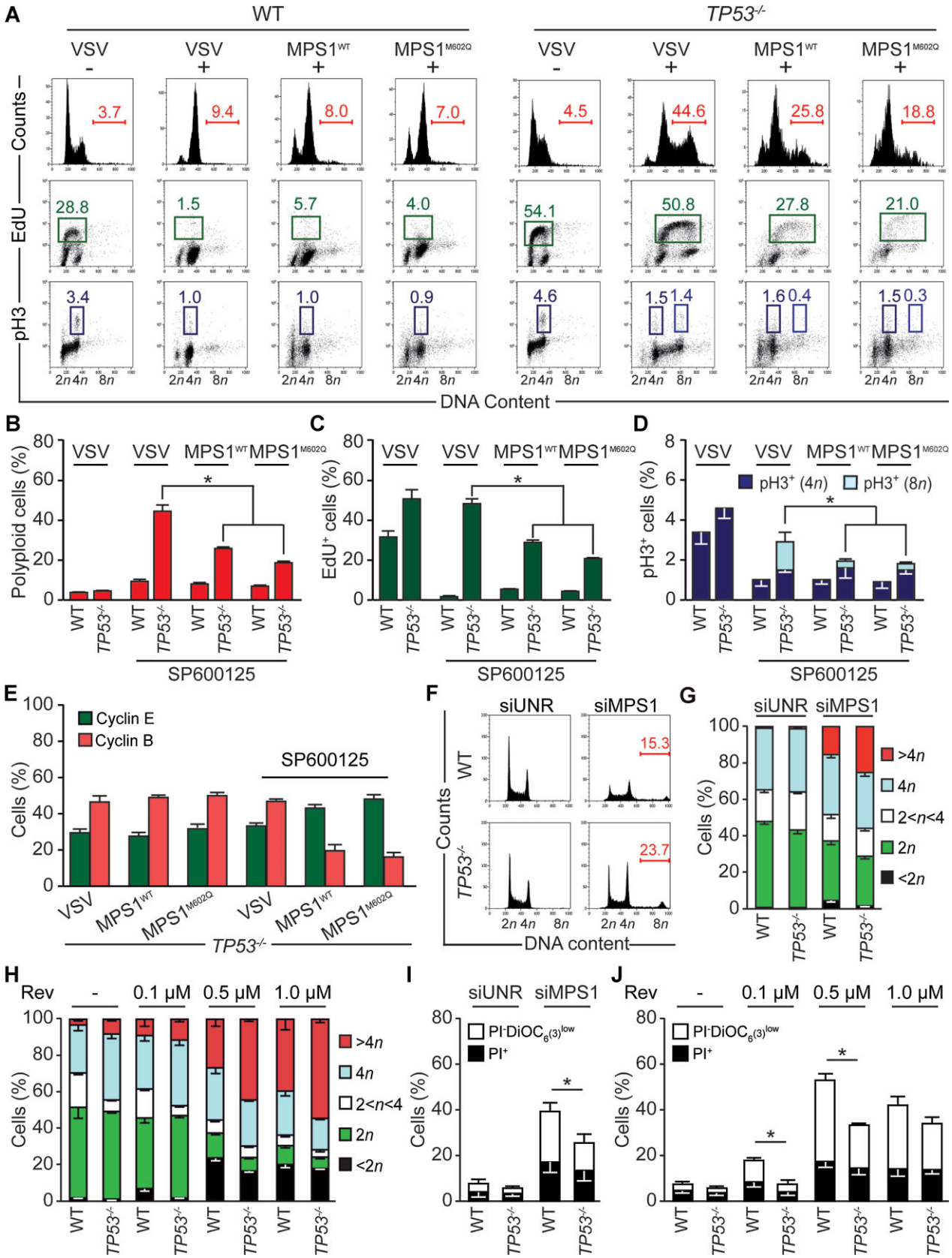

Figure 4.

© 2012 EMBO Molecular Medicine

Supporting Information). Similarly, the highly specific MPS1 inhibitor reversine (Santaguida et al, 2010) induced the preferential polyploidization of *TP53*$^{-/-}$ cells (Fig 4H). Nonetheless, depletion or inhibition of MPS1 failed to kill p53-deficient cells more efficiently than their WT counterparts (Fig 4I and J and Fig S5 of Supporting Information), suggesting that MPS1 inhibition is required but not sufficient for the selective killing of *TP53*$^{-/-}$ cells by SP600125. Finally, the preferential killing of p53-negative over p53-expressing cells was not reproduced by the selective depletion of Aurora kinase A, Aurora kinase B, CHEK1, CHEK2, FLT3, JNK1, JNK2 and MEK1 alone or in various combinations including with MPS1 (Figs S6–S8 of Supporting Information).

Mechanisms of cell death induced by SP600125

To understand the link(s) between the polyploidization of *TP53*$^{-/-}$ cells and their enhanced mortality, we performed detailed videomicroscopic analyses of histone 2B (H2B)-GFP-expressing WT and *TP53*$^{-/-}$ cells responding to SP600125 (Fig 5A). While there were no differences in the proliferative potential of untreated WT and *TP53*$^{-/-}$ cells, dramatic discrepancies became apparent upon exposure to SP600125 (Fig 5B). In the presence of SP600125, indeed, WT cells did not manifest a mitotic arrest but typically underwent one round of abortive mitosis featuring a transient phase of chromatin condensation but not a symmetric metaphase plate, followed by karyokinesis failure, no cytokinesis and either quiescence (no further mitosis) or cell death (Fig 5A and B and Video 1 of Supporting Information). In contrast, more than half of SP600125-treated *TP53*$^{-/-}$ cells underwent two consecutive rounds of abortive mitosis (in the absence of karyokinesis and cytokinesis), leading to increased nuclear size and DNA content (Fig 5A–D and Video 2 of Supporting Information). Importantly, in a significant fraction of these cells, the first or second round of abortive mitosis was followed by the activation of mitotic catastrophe and cell death (Vitale et al, 2011), which always occurred 10 h *after* from mitotic failure (and never *during* mitosis) (Fig 5A–D and Video 3 of Supporting Information). In line with these results, non-proliferating *TP53*$^{-/-}$ cells (cultured either in presence of low serum concentrations or at high confluence) were partially protected against SP600125, and their selective susceptibility to the drug was lost (Fig 6A). This finding unambiguously proves the causal link between proliferation and cell death as induced by SP600125. Clonogenic assays confirmed that SP600125 was more efficient in permanently reducing the clonogenic potential of *TP53*$^{-/-}$ cells than that of their WT counterparts (Fig 6B). This loss of proliferative capacity was accompanied by the activation of mitochondrial pathways of apoptosis, as documented by the $\Delta\psi_m$ dissipation (see above), the release of cytochrome *c* from mitochondria and the subsequent activation of caspase-3 and chromatin condensation (Fig 6C). The knockdown of pro-apoptotic proteins such as PUMA and BAX (but not BAK) reduced, while the depletion of Bcl-2-like apoptosis inhibitors (*i.e.* Bcl-2, Bcl-X_L and MCL-1) enhanced, the fraction of *TP53*$^{-/-}$ cells succumbing to SP600125 (Fig 6D). The broad-spectrum caspase inhibitor Z-VAD-fmk inhibited cell death as well as the appearance of a sub-diploid population of apoptotic bodies as induced by SP6000125 (Fig 6E).

Altogether, these results suggest that SP600125 kills *TP53*$^{-/-}$ cells secondary to one or two rounds of mitotic abortion and following the activation of the mitochondrial pathway of apoptosis. Thus, SP600125 triggers one program of mitotic catastrophe, preferentially in p53-deficient cells.

p53-deficient cancer cell killing by SP600125 *in vitro* and *in vivo*

SP600125 selectively killed *TP53*$^{-/-}$ (as opposed to WT as well as to *BAX*$^{-/-}$, *CHK2*$^{-/-}$ and *CDKN1A*$^{-/-}$) HCT 116 cells, suggesting that its effect is specific (Fig 7A). The depletion of p53 by three distinct siRNAs and the transient transfection of two dominant-negative p53 mutants (His175 and His273) sensitized WT HCT 116 cells to SP600125, mimicking the effect of gene knockout (Fig 7B and C and Fig S2D of Supporting Information). Similarly, the deletion, depletion or inhibition of p53 sensitized cell lines other than HCT 116 to SP600125. This applied to human colorectal cancer RKO cells subjected to the siRNA-mediated knockdown of p53 (Fig 7D and Fig S2E of Supporting Information), human osteosarcoma Saos-2 cells expressing p53-His273 in a doxycycline-inducible fashion (Fig 7E), human ovarian carcinoma SKOV-3 cells expressing two different variants of dominant-negative p53 (Fig 7F) and mouse embryonic fibroblasts (MEFs) lacking *Tp53* due to homologous recombination (Fig 7G). Moreover, SP600125 killed non-

Figure 4. Implication of MPS1 in the p53-dependent effects of SP600125 on the cell cycle.

A-D. Contribution of MPS1 to cell cycle progression. WT and *TP53*$^{-/-}$ human colon carcinoma HCT 116 cells were transfected with an empty vector (VSV) or with a plasmid encoding WT MPS1 or an SP600125-resistant variant of MPS1 (MPS1^{M602Q}), then left untreated (–) or treated with 30 μM SP600125 for 24 h (+) and subjected to cell cycle analysis and assessed for active DNA synthesis (by means of EdU labelling) and histone H3 phosphorylation (by immunofluorescence). Representative cell cycle distributions and scatter plots are shown in (**A**) (numbers refer to the percentage of cells found in each gate) and quantitative results (means ± SEM, $n = 3$) are reported in (**B–D**). $^*p < 0.05$ (Student's *t*-test).

E. Impact of MPS1 on cyclin B and E levels in *TP53*$^{-/-}$ HCT 116 cells. The frequency of cells expressing cyclin E (in green) or cyclin B (in red) upon transfection with the indicated plasmids and treatment with 30 μM SP600125 for 24 h was determined by immunofluorescence (means ± SEM, $n = 3$).

F-J. Effects of MPS1 depletion or inhibition on WT or *TP53*$^{-/-}$ cells. Seventy-two hours after transfection with a control siRNA (siUNR) or with a siRNA targeting MPS1 (siMPS1) (**F**, **G** and **I**) or 48 h after the administration of the indicated concentrations of reversine (Rev) (**H** and **J**), WT or *TP53*$^{-/-}$ HCT 116 cells were stained to measure DNA content (**F–H**) or cell death-related parameters (**I** and **J**). Representative cell cycle distributions are shown in (**F**) (numbers refers to the percentage of cells displaying a >4*n* DNA content), and quantitative data are reported in **G–J** (means ± SEM, $n = 6$). In (**I** and **J**), white and black columns illustrate the percentage of dying (PI^- $DiOC_6(3)^{low}$) and dead (PI^+) cells, respectively (means ± SEM; $n = 6$). $^*p < 0.05$ (Student's *t*-test), as compared to *TP53*$^{-/-}$ cells transfected with the same siRNA (**I**) or treated with the same concentration of Rev (**J**).

 © 2012 EMBO Molecular Medicine

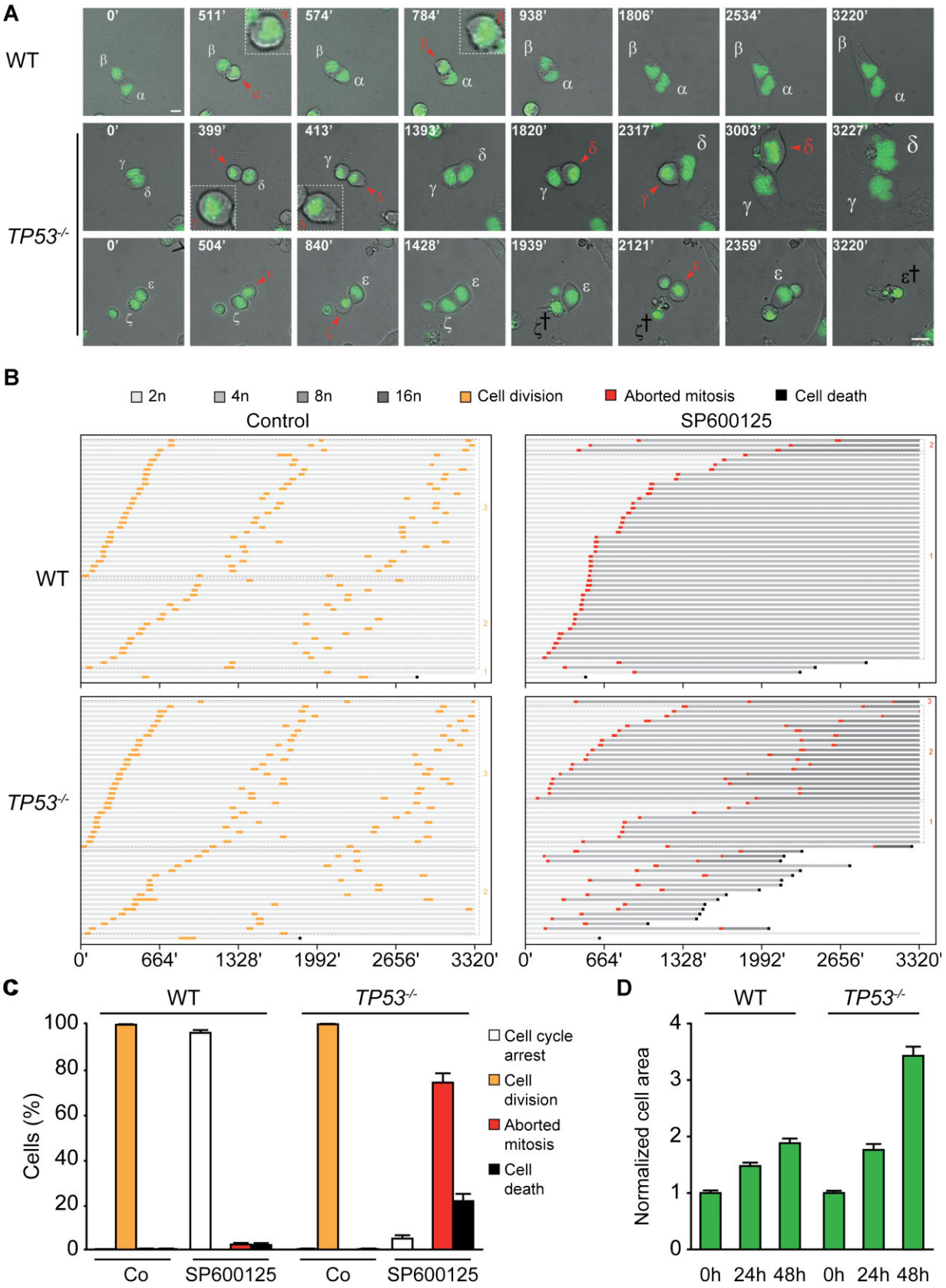

Figure 5.

© 2012 EMBO Molecular Medicine

immortalized *Tp53*$^{-/-}$ mouse adult fibroblasts (at early culture passages) more efficiently than their p53-sufficient counterparts (Fig 7H). These results suggest that the capacity of SP600125 to selectively eliminate *TP53*$^{-/-}$ cells can be generalized. Importantly, not only the absence of p53 but also the continuative presence of SP600125 is required for efficient cell death induction, confirming the notion that, in p53-deficient contexts, SP600125 promotes mitotic aberrations that activate a delayed program of mitotic catastrophe-induced cell death (Fig S9 of Supporting Information). Of note, the intraperitoneal administration of SP600125 did not affect the growth of p53-proficient WT HCT 116 tumours xenografted in athymic mice. However, the same systemic regimen was able to inhibit the growth of isogenic *TP53*$^{-/-}$ HCT 116 tumours (Fig 7I), underscoring the notion that SP600125 can mediate selective therapeutic effects against p53-deficient tumours *in vivo*.

CONCLUDING REMARKS

In this paper, we identified SP600125 as an agent that induces polyploidization and cell death preferentially in p53-deficient cells. SP600125 is a multi-kinase inhibitor (Colombo et al, 2010) and its selective toxicity on *TP53*$^{-/-}$ cells could not be recapitulated by the selective depletion of several among its most prominent pharmacological targets including JNK1, JNK2 or MPS1, alone or in combination. This is in contrast with previous results indicating that SP600125-induced cell death depends on JNK (Mingo-Sion et al, 2004) and that *TP53*$^{-/-}$ cells are sensitive to JNK2 depletion (Potapova et al, 2000). Rather, our results suggest that SP600125 mediates its cytotoxic effects via a multipronged inhibitory action on several serine/threonine kinases. Nonetheless, it appears that the inhibition of MPS1 is at least co-responsible for the preferential effects of SP600125 on the cell cycle of *TP53*$^{-/-}$ cells. Indeed, transfection with MPS1 (and more so with an SP600125-resistant mutant of MPS1) limited the polyploidization of *TP53*$^{-/-}$ cells responding to SP600125. Thus, one of (but not the sole) targets of SP600125 underlying its therapeutic profile against p53-deficient cells is MPS1. Highly specific MPS1 inhibitors are currently in preclinical and clinical development (Colombo et al, 2010; Hewitt et al, 2010; Kwiatkowski et al, 2010; Santaguida et al, 2010; Sliedrecht et al, 2010). However, there are no reports indicating that such compounds would preferentially kill p53-deficient cells. It should be noted that the simultaneous inhibition of several kinases may exert synergistic pro-apoptotic actions (Olaussen et al, 2009) and that less specific kinase inhibitors may have broader anticancer effects than highly targeted agents, as this has been determined in several clinical studies (Knight et al, 2010). Thus, the relative non-specificity of SP600125 may turn into a therapeutic advantage.

Previous groups reported that SP600125 can induce polyploidization in NIH 3T3 MEFs (Schmidt et al, 2005) and in multiple different human cancer cells, including non-small cell lung carcinoma (A549) (Miyamoto-Yamasaki et al, 2007), small lung carcinoma (Calu-1), cervical carcinoma (HeLa; MacCorkle & Tan, 2004), breast cancer (MCF-7, MDA MB-231, and 21PT) (Mingo-Sion et al, 2004), osteosarcoma (U2OS) (Kim et al, 2010) and mantle cell lymphoma cells (Wang et al, 2009). Two different mechanisms have been proposed for this effect, namely subsequent rounds of mitosis in the absence of karyokinesis and cytokinesis or, alternatively, direct endoduplication from the G_2 phase, due to the inhibition of CDK1. This latter mechanism has been described to occur in p53-sufficient cells, and has been attributed to the (indirect) inhibition of CDK1 secondary to that of Aurora kinase A and PLK1 (Kim et al, 2010). To our knowledge, no systematic studies have been performed so far to compare the efficacy of SP600125-induced polyploidization in p53-sufficient and p53-deficient cells with one exception (Kuntzen et al, 2005). In this study, upon SP600125 administration for a short time period (16 h), the authors observed no differences in cell cycle distribution and cell death activation in presence or absence of p53. At odds with this, our results suggest that p53 has a profound impact on the efficacy (and perhaps the mechanism) of polyploidization as induced by SP600125. In response to SP600125, *TP53*$^{-/-}$ cells reach higher level of ploidy than their *TP53*$^{+/+}$ counterparts, and they do so while contracting their chromosomes periodically in abortive (pro-)metaphases without forming *bona fide* metaphase plates, perhaps because centrosomes aggregate in a single cluster or they are not able to orchestrate a correct mitotic spindle. Thereafter, the chromosomes of *TP53*$^{-/-}$ cells decondense with no signs of anaphase-associated chromosomal movements and in the absence of complete chromosome separation, as indicated by FISH and live chromosome labelling. *TP53*$^{-/-}$ cells are able to go through this round of abortive mitosis up to three times in the presence of SP600125. In any of these rounds (most often in the first or second one, rarely in the third one), the mitochondrial pathway of apoptosis gets activated, most frequently with a latency of approximately 10 h after mitosis.

Figure 5. Videomicroscopic cell cycle profiling of SP600125 effects on WT and TP53$^{-/-}$ cells. WT and *TP53*$^{-/-}$ human colon carcinoma HCT 116 cells engineered to express a GFP-histone 2B fusion protein were treated with 30 μM SP600125 (time = 0 min) and then followed by live videomicroscopy for 3320 min.

A. Representative images. Greek letters refer to individual cells that underwent abortive mitosis (red labelling and arrowhead) – with transient chromatin condensation (inserts) – or apoptosis (black labelling and cross). Please note the increase in cell diameter (depicted by the increase in letter size), in particular among *TP53*$^{-/-}$ cells.

B. Cell fate profiles of untreated (control) or SP600125-treated cells with the indicated genotypes, as shown for 50 cells in each condition. Orange and red traits depict productive cell divisions and aborted mitoses, respectively. Grey darkening indicates an increase in cell ploidy.

C,D. Quantification of cell fates (**C**) or cell size increments (**D**) among WT and *TP53*$^{-/-}$ HCT 116 cells left untreated (Co) or administered with 30 μM SP600125 for 48 h (means ± SEM, $n = 100$ cells per data point). In (**C**), only cells generated by a normal or abortive mitosis within the first 300 min of the assays were tracked and quantified. Scale bar = 10 μm.

 © 2012 EMBO Molecular Medicine

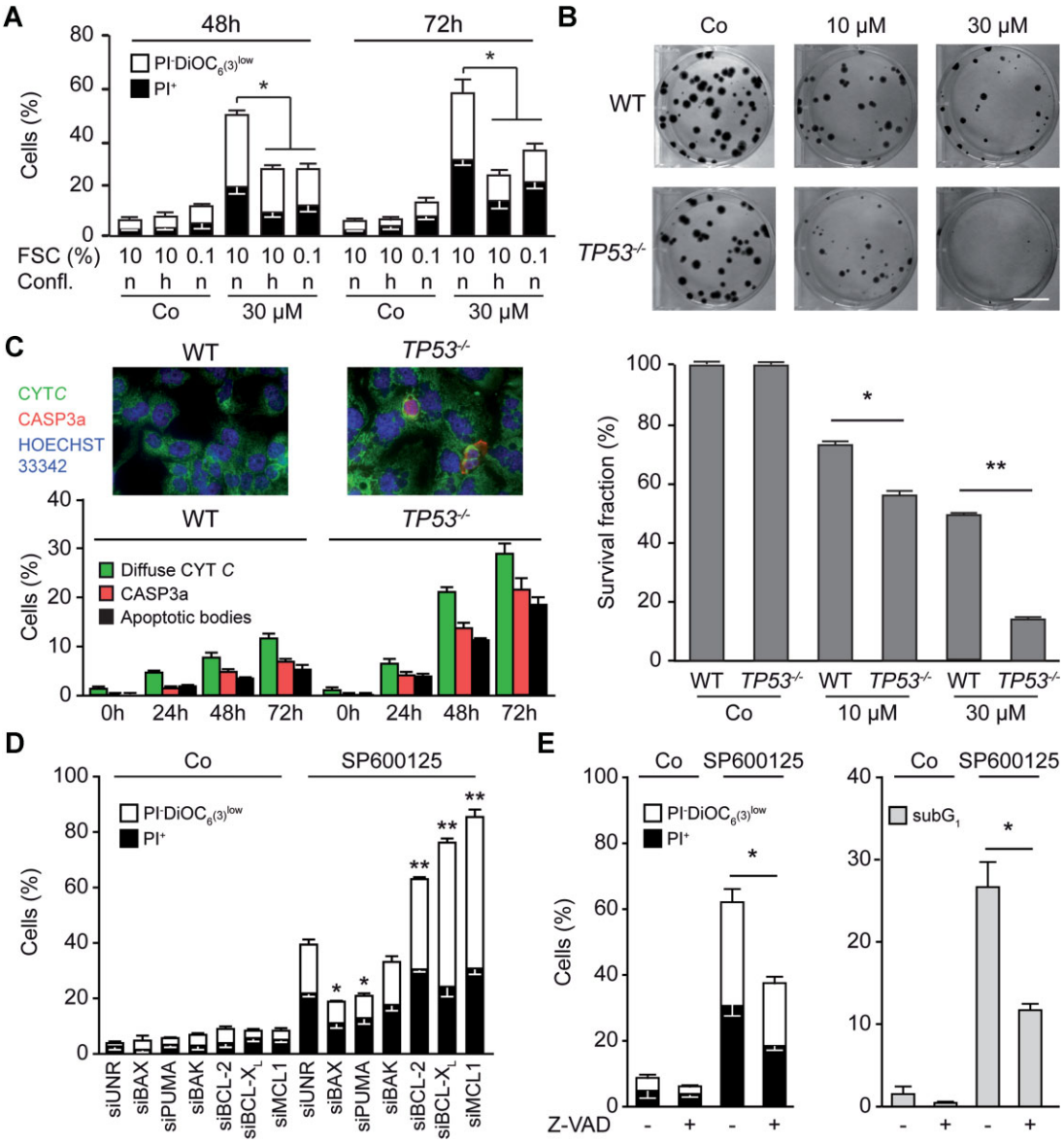

Figure 6. Mechanisms of SP600125-induced cell death in TP53$^{-/-}$ cells.

A. Impact of cell proliferation on cell death triggered by SP600125. *TP53*$^{-/-}$ colon carcinoma HCT 116 cells were maintained in the presence of in the absence of 10% foetal calf serum (FCS) or cultured at normal (*n*) or high (*h*) confluence and treated or not with 30 μM SP600125 for the indicated time, followed by cytofluorometric assessment of the cell death-related parameters (means ± SEM; $n = 4$). $^{*}p < 0.05$, (Student's *t*-test).

B. Clonogenic survival of WT and *TP53*$^{-/-}$ HCT 116 cells. Representative plates as well as quantitative data (means ± SEM, $n = 6$, upon normalization to untreated cells of the same genotype) are shown. $^{*}p < 0.05$ and $^{**}p < 0.01$ (Student's *t*-test). Scale bar = 3 cm.

C. Mitochondrial cytochrome *c* release upstream of caspase-3 activation. Cells were stained to visualize cytochrome *c* (CYTC, green fluorescence), activated caspase-3 (CASP3a, red fluorescence) and nuclei (Hoechst 33342, blue fluorescence), and the percentage of cells exhibiting diffuse (as opposed to punctuate) CYTC staining or caspase-3 activation was determined, together with the frequency of apoptotic bodies. Representative fluorescence microphotographs of WT and *TP53*$^{-/-}$ HCT 116 cells treated with 30 μM SP600125 for 72 h and quantitative results at the indicated time (means ± SEM, $n = 4$) are shown. Scale bar = 10 μm.

D. Involvement of Bcl-2-like proteins in the death of *TP53*$^{-/-}$ HCT 116 cells as induced by SP600125. Cells were subjected to siRNA-mediated depletion of the indicated proteins (siUNR = control siRNA) for 24 h, followed by the administration of 30 μM SP600125 for further 48 h and cytofluorometric assessment of cell death-related phenomena (means ± SEM; $n = 4$). $^{*}p < 0.05$ and $^{**}p < 0.01$ (Student's *t*-test), as compared to siUNR-trasnfected cells exposed to SP600125. In (**A**, **C** and **D**), white and black columns illustrate the percentage of dying (PI^{-} DiOC$_6$(3)^{low}) and dead (PI^{+}) cells, respectively.

E. Effects of Z-VAD-fmk on SP600125-induced manifestations of cell death. *TP53*$^{-/-}$ HCT 116 cells were left untreated (Co) or treated for 72 h with 30 μM SP600125 alone or in combination with 25 μM Z-VAD-fmk (Z-VAD), followed by staining with Hoechst 33342 (to assess DNA degradation to a subdiploid level, subG$_1$) or DiOC$_6$(3)/PI co-staining and cytofluorometry (means ± SEM, $n = 3$). $^{*}p < 0.05$ (Student's *t*-test).

 © 2012 EMBO Molecular Medicine

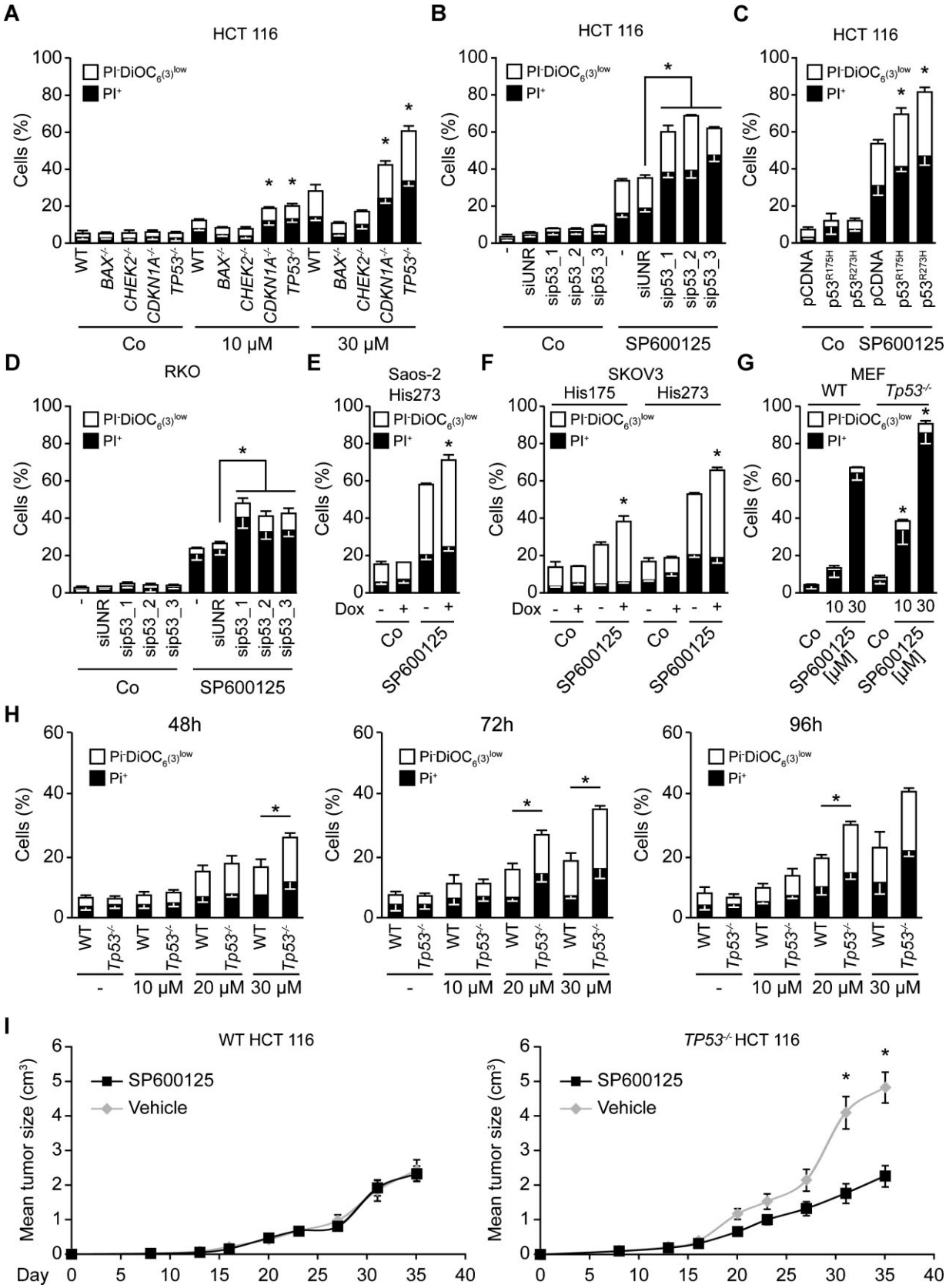

Figure 7.

 © 2012 EMBO Molecular Medicine

Thus, the killing of *TP53*$^{-/-}$ cells triggered by SP600125 is closely coupled to abortive mitosis, indicating that SP600125 constitutes a novel inducer of mitotic catastrophe (Vitale et al, 2011). Future studies must decipher the mechanisms that link SP600125-induced abortive mitosis to apoptosis, and address the potential clinical utility of this agent.

MATERIALS AND METHODS

Unless otherwise indicated, media and supplements for cell culture were purchased from Gibco-Invitrogen (Carlsbad, CA, USA) and plasticware from Corning B.V. Life Sciences (Corning, NY, USA).

Chemicals

SP600125 (anthra [1,9-cd] pyrazole-6 (2H)-one) was purchased from Sigma–Aldrich (St Louis, MO, USA) and stocked as a 30 mM solution in DMSO. Reversine (2-(4-orpholinoanilino)-6-cyclohexylaminopurine) was purchased from Calbiochem (San Diego, CA, USA) and stocked as a 10 mM solution in DMSO. The pan-caspase inhibitor *N*-benzyloxy-carbonyl-Val-Ala-Asp.fluoromethylketone (z-VAD-fmk) was obtained from Bachem Bioscience (Bubendorf, Switzerland) and stocked as a 50 mM solution in DMF. The appropriate amount of DMSO and/or DMF was always employed for negative control conditions.

Compound screen

A total of 4×10^4 WT HCT 116 cells stably expressing H2B-GFP and *TP53*$^{-/-}$ HCT 116 cells stably expressing H2B-RFP were seeded at a ratio of 1:1 in Black/Clear 96-well Imaging Plates (BD Biosciences, San Diego, CA, USA). Twenty-four hours later, cells were treated with the agents from the ICCB Known Bioactives Library (Enzo Life Sciences Inc., Farmingdale, NY, USA) at final concentrations ranging from 1 to 12 μM and kept in a Cytomat 2c automated incubator (Thermo Fisher Scientific, Waltham, MA, USA). Every 6 h, plates were instantly transferred to a BD Pathway 855 automated microscope (BD Biosciences) by means of a robotized Twister II plate handler (Caliper Life Sciences, Hopkinton, MA, USA), and four view fields in the centre of each well were acquired using a 20X objective (Olympus, Center Valley, PA, USA), for a total assay time of 48 h. Images were analysed for cell density and fluorescence intensity with the BD Attovision software (BD Biosciences) and the slope of growth curves of each subpopulation over 48 h was calculated by using the linear regression function of Microsoft Excel (Microsoft Co., Redmond, WA, USA).

RNA interference

Custom-designed siRNAs targeting MPS1 (siMPS1_1 sense 5′-CCCA-GAGGACUGGUUGAGUdTdT-3′; siMPS1_2 sense 5′-GCAACCACUUAUG-GUACUGdTdT-3′; siMPS1_3 sense 5′-GCACGUGACUACUUUCAAAdTdT-3′) (Stucke et al, 2004; Xu et al, 2009), p53 (sip53_1 sense 5′-GACUCCAGUGGUAAUCUACdTdT-3′; sip53_2 sense 5′-GCAUGAACCG-GAGGCCCAUdTdT-3′; sip53_3 sense 5′-CUACUUCCUGAAAACAACGdTdT-3′) (Gu et al, 2004; Martinez et al, 2002), AURKB (5′-GGAGGAGGAU-CUACUUGAUTT-3′), CHEK1 (sense 5′-UCGUGAGCGUUUGUUGAACTT-3′), CHEK2 (sense 5′-UGUGUGAAUGACAACUACUTT-3′), Bcl-2 (Vicencio et al, 2009), Bcl-X_L (de La Motte Rouge et al, 2007), MCL1 (Kepp et al, 2009) and PUMA (Vitale et al, 2007), were purchased from Sigma-Proligo (The Woodlands, TX, USA).

Alternatively, siRNA duplexes for the downregulation of FLT3 and MPS1 (siGENOME Smart-pool M-003137 and M-004105, respectively), were purchased from Dharmacon (Chicago, IL, USA), siRNAs targeting JNK1 (sc-29380) from Santa Cruz (Santa Cruz Biotechnology Inc., Santa Cruz, CA, USA), siRNAs for the down-regulation of AURKA, JNK2 and MEK1 (SIHK0142, SIHK1224 and SIHK1098, respectively), from Sigma–Aldrich and siRNAs for the down-regulation of BAK1 and BAX (Hs_BAK1_5 and Hs_BAX_10 HP Validated siRNAs, respectively) from Qiagen (Hilden, Germany) (de La Motte Rouge et al, 2007). As a control, a non-targeting siRNA with a sequence unrelated to the human genome was used (UNR, sense 5′-GCCGGUAUGCCGGUUAAGUdTdT-3′).

Cells pre-seeded in 12-well plates were transfected with plasmids at 80% confluence by means of the Attractene Transfection reagent (Qiagen) as recommended by the manufacturer, or with siRNAs at 30–40% confluence by means of the HiPerFect® transfection reagent (Qiagen), as previously described (Hoffmann et al, 2008). After 48 or 72 h, transfection efficiency was determined by immunoblotting.

Immunofluorescence and videomicroscopy

Immunofluorescence microscopy determinations were performed as previously described (Vitale et al, 2007, 2008). For videomicroscopy,

Figure 7. Effects of the deletion depletion or inhibition of p53 on SP600125 cytotoxicity in several cell lines.

A–H. Lethal effects of SP600125 on p53-deficient cancer cells *in vitro*.

A–C. Human colon carcinoma HCT 116 cells with different knockout genotypes (**A**), subjected to the transient depletion of p53 (for 24 h) with three distinct siRNAs (**B**) or transiently transfected (for 24 h) with dominant-negative p53 mutants (His175 and His273) (**C**) were left untreated or treated with SP600125 for 72 h as illustrated (30 μM where not specified).

D–F. Alternatively human colon carcinoma RKO cells subjected to the siRNA-mediated knockdown of p53 (**D**), human osteosarcoma Saos-2 cells (**E**) or human ovarian carcinoma SKOV-3 cells (**F**) expressing doxycycline (Dox)-inducible p53 mutants cultured for 1 week in the absence or presence of Dox were kept in control conditions or treated with 30 μM SP600125 for 72 h.

G,H. Similarly, MEFs (**G**) or early passage mouse adult fibroblasts (AFs) obtained from the ears mice of the indicated genotype (**H**) were compared for their susceptibility to SP600125-induced killing. In all cases (**A–H**), $DiOC_6(3)$/PI co-staining and cytofluorometric analysis were performed to assess cell death-related variables. White and black columns illustrate the percentage of dying (PI^- $DiOC_6(3)^{low}$) and dead (PI^+) cells, respectively (means ± SEM, $n = 3$). siUNR, control siRNA. $^*p < 0.05$ (Student's *t*-test), as compared to WT cells (**A** and **G**) cells transfected with the empty vector pCDNA (**C**), cells not exposed to Dox (**E** and **F**), treated with the same concentration of SP600125.

I. *In vivo* growth arrest of p53-deficient tumours by SP600125. WT or *TP53*$^{-/-}$ HCT 116 cells were injected subcutaneously into athymic mice (30 mice for SP600125-treated groups, 15 mice for vehicle-treated controls), and 1 week later intraperitoneal injections of SP600125 were performed, as described in Materials and Methods Section. Tumour size was then routinely monitored by means of a common calliper. Results are reported as means ± SEM. $^*p < 0.05$ (two-tailed Student's *t*-test), as compared to vehicle-treated mice.

 © 2012 EMBO Molecular Medicine

The paper explained

PROBLEM:

p53 is the tumour suppression protein whose function is most frequently lost in human cancer. Thus, more than 20 million people worldwide live with cancers in which p53 is mutated or the p53 pathway is interrupted due to the inactivation of molecules that act either upstream or downstream of p53. The loss of p53 reduces the efficacy of several conventional anticancer agents, meaning that p53-deficient tumours are intrinsically chemoresistant. This work has been designed to identify small molecules that preferentially kill cancer cells lacking p53 expression or expressing a mutated p53 variant.

RESULTS:

A screen in which p53-sufficient and p53-deficient tumour cells were systematically compared for their response to known or experimental anticancer agents led to the identification of one molecule, SP600125, that killed p53-deficient cells more efficiently than their p53-expressing counterparts. This property of SP600125 was validated on multiple cell lines that differed relative to the function of the p53 system. In particular, we found that human p53-deficient cancer cells growing on immunodeficient mice responded to chemotherapy with SP600125 in conditions in which similar cancer cells that express intact p53 failed to do so. We characterized the mechanisms through which SP600125 can kill p53-deficient (but not p53-sufficient) cancer cells. We found that p53-sufficient cells underwent a cell cycle arrest upon exposure to SP600125 and ultimately survived. In contrast, p53-deficient cells exposed to SP600125 undertook a series of abortive mitoses (featuring karyokinesis but no cytokinesis), eventually generating giant cells that finally underwent apoptotic cell death.

IMPACT:

Altogether, these results delineate a novel strategy to selectively target cells that lack functional p53. SP600125 exemplifies a class of drugs that kill p53-deficient cells in a preferential fashion, based on the incapacity of such cells to undergo a cell cycle arrest in particular circumstances. Hence, SP600125 (and its analogues/derivatives) might be used for cancer chemoprevention (for eliminating pre-malignant cells that have inactivated p53) or chemotherapy of p53-deficient cancers.

HCT 116 cells stably expressing a H2B-GFP fusion were grown in 96-well imaging plates (BD Biosciences) under standard culture conditions and subjected to pulsed observations (every 7 min for up to 48 h) with a BD pathway 855 automated live cell microscope (BD Biosciences). Images were analysed with the open source software Image J. Cell fate profile are illustrated as previously published (Rello-Varona et al, 2010).

In vivo xenograft models

Athymic *nu/nu* female mice (age ~42 days, body weight ~20 g, provided by the Institut Gustave Roussy, Villejuif, France in-house animal facility) were used throughout this study in strict compliance with widely accepted ethical guidelines for animal experimentation. Mice were kept in Makrolons type III wire mesh laboratory cages (Charles River, Boston, MA, USA), under poor germ conditions at 24°C and 50–60% humidity, and were allowed for food and water *ad libitum*. Light cycle was artificially controlled to provide 14 h of light (from 06:30 a.m. to 08:30 p.m.). After 4 days of acclimation period, mice were subcutaneously xenografted with 2×10^6 WT or *TP53*$^{-/-}$ HCT 116 cells (Vitale et al, 2007). After 1 week, mice were injected i.p. with 5 mg/kg SP600125 (or an equivalent volume of vehicle) every 2–3 days. Due to its limited solubility in water, SP600125 was injected in 2% DMSO, 2% polyethylene glycol 600 (PEG600) and 2% Tween 80 in PBS. Statistical analyses were carried out by means of the SigmaStat package (Systat Software, San Jose, CA, USA). Statistical significance was determined by means of two-tailed unpaired Student's *t*-test ($^{*}p < 0.05$) in the context of a pairwise comparison procedure.

Statistical procedures

Unless otherwise specified, all experiments were carried out in triplicate parallel instances and independently repeated at least three times. Data were analysed with Microsoft Excel (Microsoft) and statistical significance was assessed by means of two-tailed unpaired Student's *t*-test ($^{*}p < 0.05$; $^{**}p < 0.001$).

The complete set of experimental and statistical procedures can be found online as Supporting Information.

Author contributions

MJ, OK, FB, LS, GM, SAM, SRV, DL, AA, MT, FS, FH, GP and MC designed and performed experiments and analysed data; IV designed and performed experiments, analysed data and wrote the paper; LG designed experiments and wrote the paper; GK designed experiments, wrote the paper and directed biological studies.

Acknowledgements

We are indebted to Bert Vogelstein for WT and *TP53*$^{-/-}$ HCT 116 cells, Tyler Jacks for MEF cells and Duane A. Compton for HCT 116 cells with a single GFP-labelled chromosome. We thank Klas Wiman for the generous gift of cell lines expressing inducible p53 mutants. We acknowledge the kind gift of cDNAs encoding MPS1 by Rene Medema and of p53 dominant negatives mutants by Dr. Thierry Soussi. We thank Caterina Tanzarella for the help in the design of interphase FISH experiment and for the critical reading of the manuscript. IV is

 © 2012 EMBO Molecular Medicine

supported by the Ligue Nationale contre le Cancer, SRV by the Fondation de France and LG from Apo-Sys and SAM by the Higher Education Commission (HEC) of Pakistan. This work was supported by grants to GK from the Ligue Nationale contre le Cancer (Equipe labellisée), Agence Nationale pour la Recherche (ANR), European Commission (Active p53, Apo-Sys, ChemoRes, ApopTrain), Fondation pour la Recherche Médicale (FRM), Institut National du Cancer (INCa), Cancéropôle Ile-de-France, Fondation Bettencourt-Schueller and the LabEx Onco-Immunology.

Supporting Information is available at EMBO Molecular Medicine online.

The authors declare that they have no conflict of interest.

References

Athar M, Elmets CA, Kopelovich L (2011) Pharmacological activation of p53 in cancer cells. Curr Pharm Des 17: 631-639

Aylon Y, Michael D, Shmueli A, Yabuta N, Nojima H, Oren M (2006) A positive feedback loop between the p53 and Lats2 tumor suppressors prevents tetraploidization. Genes Dev 20: 2687-2700

Beckerman R, Prives C (2010) Transcriptional regulation by p53. Cold Spring Harb Perspect Biol 2: a000935

Bennett BL, Sasaki DT, Murray BW, O'Leary EC, Sakata ST, Xu W, Leisten JC, Motiwala A, Pierce S, Satoh Y, *et al* (2001) SP600125, an anthrapyrazolone inhibitor of Jun N-terminal kinase. Proc Natl Acad Sci USA 98: 13681-13686

Brown CJ, Lain S, Verma CS, Fersht AR, Lane DP (2009) Awakening guardian angels: drugging the p53 pathway. Nat Rev Cancer 9: 862-873

Castedo M, Ferri K, Roumier T, Metivier D, Zamzami N, Kroemer G (2002) Quantitation of mitochondrial alterations associated with apoptosis. J Immunol Methods 265: 39-47

Castedo M, Coquelle A, Vivet S, Vitale I, Kauffmann A, Dessen P, Pequignot MO, Casares N, Valent A, Mouhamad S, *et al* (2006) Apoptosis regulation in tetraploid cancer cells. EMBO J 25: 2584-2595

Cheok CF, Verma CS, Baselga J, Lane DP (2011) Translating p53 into the clinic. Nat Rev Clin Oncol 8: 25-37

Chu ML, Chavas LM, Douglas KT, Eyers PA, Tabernero L (2008) Crystal structure of the catalytic domain of the mitotic checkpoint kinase Mps1 in complex with SP600125. J Biol Chem 283: 21495-21500

Colombo R, Caldarelli M, Mennecozzi M, Giorgini ML, Sola F, Cappella P, Perrera C, Depaolini SR, Rusconi L, Cucchi U, *et al* (2010) Targeting the mitotic checkpoint for cancer therapy with NMS-P715, an inhibitor of MPS1 kinase. Cancer Res 70: 10255-10264

Davoli T, de Lange T (2011) The causes and consequences of polyploidy in normal development and cancer. Annual Rev Cell Dev Biol 27: 585-610

de La Motte Rouge T, Galluzzi L, Olaussen KA, Zermati Y, Tasdemir E, Robert T, Ripoche H, Lazar V, Dessen P, Harper F, *et al* (2007) A novel epidermal growth factor receptor inhibitor promotes apoptosis in non-small cell lung cancer cells resistant to erlotinib. Cancer Res 67: 6253-6262

Degenhardt Y, Greshock J, Laquerre S, Gilmartin AG, Jing J, Richter M, Zhang X, Bleam M, Halsey W, Hughes A, *et al* (2010) Sensitivity of cancer cells to Plk1 inhibitor GSK461364A is associated with loss of p53 function and chromosome instability. Mol Cancer Ther 9: 2079-2089

Finkin S, Aylon Y, Anzi S, Oren M, Shaulian E (2008) Fbw7 regulates the activity of endoreduplication mediators and the p53 pathway to prevent drug-induced polyploidy. Oncogene 27: 4411-4421

Galluzzi L, Zamzami N, de La Motte Rouge T, Lemaire C, Brenner C, Kroemer G (2007) Methods for the assessment of mitochondrial membrane permeabilization in apoptosis. Apoptosis 12: 803-813

Galluzzi L, Aaronson SA, Abrams J, Alnemri ES, Andrews DW, Baehrecke EH, Bazan NG, Blagosklonny MV, Blomgren K, Borner C, *et al* (2009) Guidelines for the use and interpretation of assays for monitoring cell death in higher eukaryotes. Cell Death Differ 16: 1093-1107

Galluzzi L, Morselli E, Kepp O, Vitale I, Pinti M, Kroemer G (2011a) Mitochondrial liaisons of p53. Antioxid Redox Signal 15: 1691-1714

Galluzzi L, Senovilla L, Vitale I, Michels J, Martins I, Kepp O, Castedo M, Kroemer G (2011b) Molecular mechanisms of cisplatin resistance. Oncogene, DOI: 10.1038/onc.2011.384

Ganem NJ, Storchova Z, Pellman D (2007) Tetraploidy, aneuploidy and cancer. Current Opin Genet Dev 17: 157-162

Gizatullin F, Yao Y, Kung V, Harding MW, Loda M, Shapiro GI (2006) The Aurora kinase inhibitor VX-680 induces endoreduplication and apoptosis preferentially in cells with compromised p53-dependent postmitotic checkpoint function. Cancer Res 66: 7668-7677

Green DR, Kroemer G (2009) Cytoplasmic functions of the tumour suppressor p53. Nature 458: 1127-1130

Gu J, Zhang L, Swisher SG, Liu J, Roth JA, Fang B (2004) Induction of p53-regulated genes in lung cancer cells: implications of the mechanism for adenoviral p53-mediated apoptosis. Oncogene 23: 1300-1307

Ha GH, Baek KH, Kim HS, Jeong SJ, Kim CM, McKeon F, Lee CW (2007) p53 activation in response to mitotic spindle damage requires signaling via BubR1-mediated phosphorylation. Cancer Res 67: 7155-7164

Heo YS, Kim SK, Seo CI, Kim YK, Sung BJ, Lee HS, Lee JI, Park SY, Kim JH, Hwang KY, *et al* (2004) Structural basis for the selective inhibition of JNK1 by the scaffolding protein JIP1 and SP600125. EMBO J 23: 2185-2195

Hewitt L, Tighe A, Santaguida S, White AM, Jones CD, Musacchio A, Green S, Taylor SS (2010) Sustained Mps1 activity is required in mitosis to recruit O-Mad2 to the Mad1-C-Mad2 core complex. J Cell Biol 190: 25-34

Hoffmann J, Vitale I, Buchmann B, Galluzzi L, Schwede W, Senovilla L, Skuballa W, Vivet S, Lichtner RB, Vicencio JM, *et al* (2008) Improved cellular pharmacokinetics and pharmacodynamics underlie the wide anticancer activity of sagopilone. Cancer Res 68: 5301-5308

Kepp O, Gottschalk K, Churin Y, Rajalingam K, Brinkmann V, Machuy N, Kroemer G, Rudel T (2009) Bim and Bmf synergize to induce apoptosis in Neisseria gonorrhoeae infection. PLoS Pathog 5: e1000348

Kim JA, Lee J, Margolis RL, Fotedar R (2010) SP600125 suppresses Cdk1 and induces endoreplication directly from G2 phase, independent of JNK inhibition. Oncogene 29: 1702-1716

Knight ZA, Lin H, Shokat KM (2010) Targeting the cancer kinome through polypharmacology. Nat Rev Cancer 10: 130-137

Kuntzen C, Sonuc N, De Toni EN, Opelz C, Mucha SR, Gerbes AL, Eichhorst ST (2005) Inhibition of c-Jun-N-terminal-kinase sensitizes tumor cells to CD95-induced apoptosis and induces G2/M cell cycle arrest. Cancer Res 65: 6780-6788

Kwiatkowski N, Jelluma N, Filippakopoulos P, Soundararajan M, Manak MS, Kwon M, Choi HG, Sim T, Deveraux QL, Rottmann S, *et al* (2010) Small-molecule kinase inhibitors provide insight into Mps1 cell cycle function. Nat Chem Biol 6: 359-368

Levesque AA, Kohn EA, Bresnick E, Eastman A (2005) Distinct roles for p53 transactivation and repression in preventing UCN-01-mediated abrogation of DNA damage-induced arrest at S and G2 cell cycle checkpoints. Oncogene 24: 3786-3796

MacCorkle RA, Tan TH (2004) Inhibition of JNK2 disrupts anaphase and produces aneuploidy in mammalian cells. J Biol Chem 279: 40112-40121

Martinez LA, Naguibneva I, Lehrmann H, Vervisch A, Tchenio T, Lozano G, Harel-Bellan A (2002) Synthetic small inhibiting RNAs: efficient tools to inactivate oncogenic mutations and restore p53 pathways. Proc Natl Acad Sci USA 99: 14849-14854

Mingo-Sion AM, Marietta PM, Koller E, Wolf DM, Van Den Berg CL (2004) Inhibition of JNK reduces G2/M transit independent of p53, leading to

 © 2012 EMBO Molecular Medicine

endoreduplication, decreased proliferation, and apoptosis in breast cancer cells. Oncogene 23: 596-604

Miyamoto-Yamasaki Y, Yamasaki M, Tachibana H, Yamada K (2007) Induction of endoreduplication by a JNK inhibitor SP600125 in human lung carcinoma A 549 cells. Cell Biol Int 31: 1501-1506

Olaussen KA, Commo F, Tailler M, Lacroix L, Vitale I, Raza SQ, Richon C, Dessen P, Lazar V, Soria JC, *et al* (2009) Synergistic proapoptotic effects of the two tyrosine kinase inhibitors pazopanib and lapatinib on multiple carcinoma cell lines. Oncogene 28: 4249-4260

Potapova O, Gorospe M, Dougherty RH, Dean NM, Gaarde WA, Holbrook NJ (2000) Inhibition of c-Jun N-terminal kinase 2 expression suppresses growth and induces apoptosis of human tumor cells in a p53-dependent manner. Mol Cell Biol 20: 1713-1722

Rello-Varona S, Kepp O, Vitale I, Michaud M, Senovilla L, Jemaa M, Joza N, Galluzzi L, Castedo M, Kroemer G (2010) An automated fluorescence videomicroscopy assay for the detection of mitotic catastrophe. Cell Death Dis 1: e25

Santaguida S, Tighe A, D'Alise AM, Taylor SS, Musacchio A (2010) Dissecting the role of MPS1 in chromosome biorientation and the spindle checkpoint through the small molecule inhibitor reversine. J Cell Biol 190: 73-87

Schmidt M, Budirahardja Y, Klompmaker R, Medema RH (2005) Ablation of the spindle assembly checkpoint by a compound targeting Mps1. EMBO Rep 6: 866-872

Selivanova G (2010) Therapeutic targeting of p53 by small molecules. Semin Cancer Biol 20: 46-56

Shangary S, Wang S (2009) Small-molecule inhibitors of the MDM2-p53 protein-protein interaction to reactivate p53 function: a novel approach for cancer therapy. Annu Rev Pharmacol Toxicol 49: 223-241

Shen H, Moran DM, Maki CG (2008) Transient nutlin-3a treatment promotes endoreduplication and the generation of therapy-resistant tetraploid cells. Cancer Res 68: 8260-8268

Sliedrecht T, Zhang C, Shokat KM, Kops GJ (2010) Chemical genetic inhibition of Mps1 in stable human cell lines reveals novel aspects of Mps1 function in mitosis. PLoS ONE 5: e10251

Stucke VM, Baumann C, Nigg EA (2004) Kinetochore localization and microtubule interaction of the human spindle checkpoint kinase Mps1. Chromosoma 113: 1-115

Sur S, Pagliarini R, Bunz F, Rago C, Diaz LA, Jr., Kinzler KW, Vogelstein B, Papadopoulos N (2009) A panel of isogenic human cancer cells suggests a therapeutic approach for cancers with inactivated p53. Proc Natl Acad Sci USA 106: 3964-3969

Talos F, Moll UM (2010) Role of the p53 family in stabilizing the genome and preventing polyploidization. Adv Exp Med Biol 676: 73-91

Thompson SL, Compton DA (2010) Proliferation of aneuploid human cells is limited by a p53-dependent mechanism. J Cell Biol 188: 369-381

Tritarelli A, Oricchio E, Ciciarello M, Mangiacasale R, Palena A, Lavia P, Soddu S, Cundari E (2004) p53 localization at centrosomes during mitosis and postmitotic checkpoint are ATM-dependent and require serine 15 phosphorylation. Mol Biol Cell 15: 3751-3757

Vicencio JM, Ortiz C, Criollo A, Jones AW, Kepp O, Galluzzi L, Joza N, Vitale I, Morselli E, Tailler M, *et al* (2009) The inositol 1,4,5-trisphosphate receptor regulates autophagy through its interaction with Beclin 1. Cell Death Differ 16: 1006-1017

Vitale I, Galluzzi L, Vivet S, Nanty L, Dessen P, Senovilla L, Olaussen KA, Lazar V, Prudhomme M, Golsteyn RM, *et al* (2007) Inhibition of Chk1 kills tetraploid tumor cells through a p53-dependent pathway. PLoS ONE 2: e1337

Vitale I, Senovilla L, Galluzzi L, Criollo A, Vivet S, Castedo M, Kroemer G (2008) Chk1 inhibition activates p53 through p38 MAPK in tetraploid cancer cells. Cell Cycle 7: 1956-1961

Vitale I, Senovilla L, Jemaa M, Michaud M, Galluzzi L, Kepp O, Nanty L, Criollo A, Rello-Varona S, Manic G, *et al* (2010) Multipolar mitosis of tetraploid cells: inhibition by p53 and dependency on Mos. EMBO J 29: 1272-1284

Vitale I, Galluzzi L, Castedo M, Kroemer G (2011) Mitotic catastrophe: a mechanism for avoiding genomic instability. Nat Rev Mol Cell Biol 12: 385-392

Vousden KH, Prives C (2009) Blinded by the light: The growing complexity of p53. Cell 137: 413-431

Vousden KH, Ryan KM (2009) p53 and metabolism. Nat Rev Cancer 9: 691-700

Wang M, Atayar C, Rosati S, Bosga-Bouwer A, Kluin P, Visser L (2009) JNK is constitutively active in mantle cell lymphoma: cell cycle deregulation and polyploidy by JNK inhibitor SP600125. J Pathol 218: 95-103

Wiman KG (2010) Pharmacological reactivation of mutant p53: from protein structure to the cancer patient. Oncogene 29: 4245-4252

Xu Q, Zhu S, Wang W, Zhang X, Old W, Ahn N, Liu X (2009) Regulation of kinetochore recruitment of two essential mitotic spindle checkpoint proteins by Mps1 phosphorylation. Mol Biol Cell 20: 10-20

 © 2012 EMBO Molecular Medicine